RT&A, No 4 (89)
Volume 20, December 2025

SINE LOG-LOGISTIC DISTRIBUTION FOR MODELING REMISSION AND SURVIVAL TIMES OF CANCER PATIENTS

Santanu Dutta, Aditya Kumar Yadav

•

Department of Mathematical Sciences, Tezpur University, India
sdutta@tezu.ernet.in, adityakumaryadav448@gmail.com

Abstract

Modeling the remission times of bladder cancer patients reported by Lee and Wang [26], the survival times following radiotherapy and chemotherapy of head and neck cancer patients and bone cancer patients reported by Efron [10] and Mansour et al. [16] have attracted considerable research interest. In this paper, we propose a new two-parameter distribution that fits these data well and compares well in model selection for these data with existing distributions that use three or more parameters. Its distribution, density, quantile, and hazard functions have closed-form expressions. The survival function of the proposed model exhibits a regularly varying tail, and its hazard function is either strictly decreasing or inverse-bathtub shaped, depending on the value of the shape parameter. We derive several properties of the proposed distribution, estimate its parameters, and demonstrate its effectiveness in modeling the hazard function and uncovering key features of the remission time and survival time data.

Keywords: Lifetime distribution, parsimonious transformation, log-logistic distribution

1. Introduction

Cancer remains one of the leading causes of death globally, and the analysis of time-to-event data plays a crucial role in understanding treatment outcomes and disease progression. Two such important metrics in cancer research are remission time and survival time. Remission time of a disease refers to the period during which there are no symptoms of the disease following treatment [8, 26]. Survival time refers to the length of time patients live after receiving cancer treatment, such as radiotherapy, chemotherapy, or a combination of both.

Modeling remission and survival times of cancer patients has been an area of active and ongoing research (see, for instance, [1, 2, 5, 6, 11, 13, 22, 21, 23, 27] and references therein). These time-to-event data often exhibit complex features, including right-censoring, skewness, high kurtosis, and sparsity in the tail. Moreover, the underlying distributions may not conform to classical parametric families such as exponential or Weibull, motivating the development of flexible, generalized probability models.

Three publicly available datasets have been widely studied in this context. Lee and Wang [26] reported remission times (in months) of 128 bladder cancer patients. Efron [10] provided survival times (in days) of 44 head and neck cancer patients treated with a combination of radiotherapy and chemotherapy. Mansour et al. [16] reported survival times (in days) of 73 patients with acute bone cancer. Figures 1,2, and 3 show the histograms and kernel density estimates (KDEs) of these datasets, while Table 1 presents their moment coefficients of skewness and kurtosis.

All three datasets display significant positive skewness, high kurtosis, and sparsity in the right tail-indicated by the presence of a few very high values far from the central peak, which manifest

DOI: https://doi.org/10.24412/1932-2321-2025-489-216-237

as extended right tail in the KDE plots. These characteristics highlight the need for probability distributions that can capture the observed features in these data. In recent years, several probability distributions have been proposed specifically to model such datasets. For example, the remission time data of bladder cancer patients has been modeled using the WC-Weibull distribution [21], EPham distribution [1], EOEHL-LLoGP distribution [27], KGIL distribution [22], EHL-LLoGW distribution [6], GKME distribution [13], APTEPL distribution [11], Maxwell-Lomax distribution [2], RB-TL-TII-EHL-W distribution [23], and the Marshall-Olkin extended generalized Lindley (MOEGL) distribution [5]. Among these, the MOEGL distribution has demonstrated the best overall fit according to various model selection criteria.

For the survival times of 44 head and neck cancer patients, as reported by Efron [10], several recent distributions have been employed, including the power-weighted Sujatha (PWS) distribution by Shanker and Shukla [28], the gamma-Sujatha (G-SU) distribution by Ray and Shanker [19], the DUS-Inverse Weibull (DUS-IW) distribution by Gauthami and Chacko [12], and the Alpha Power Kumaraswamy Weibull (APKumW) distribution by Klakattawi [14]. Notably, the G-SU and APKumW distributions have also been applied to model survival times of acute bone cancer, as reported by Mansour et al. [16].

An appropriate probability distribution for remission or survival time enables the modeling of the hazard function $h(x)$, which represents the instantaneous rate of relapse or death-at a given time x, given that a patient is in remission or survives up to x and for small Δx, $h(x)\Delta x$ is an approximation of the chance of relapse or death in $[x, x + \Delta x)$, given survival up to x (see [25]). In cancer studies of survival time after treatment, the hazard function is expected to first increase to a peak and then decrease, exhibiting an inverse bathtub shape (see [25]) and its peak represents the time where the rate of recurrence of the disease or death is maximum, given survival up to that time, which can be crucial for treatment planning and post-treatment monitoring. For instance, in breast cancer, hazard rates often peak within the first few years following treatment, guiding the scheduling of follow-up visits and adjuvant therapies (see [7]).

In this paper, we propose a new two-parameter continuous probability distribution that provides a good fit-with high p-values under the Kolmogorov-Smirnov (KS) goodness-of-fit test-to the three datasets, viz., remission times of bladder cancer patients ([26]), and survival times of patients with head and neck cancer ([10]) and bone cancer ([16]). The proposed distribution captures the key empirical features of these datasets and compares favorably with existing models for remission or survival time across multiple model selection criteria. In addition, it yields a simple closed-form expression for the hazard function, which increases to a peak and subsequently declines with time. This pattern suggests that patients who remain in remission or survive beyond the peak hazard point have a reduced risk of cancer relapse. Importantly, the ability to identify the timing of the peak hazard can aid clinicians in planning timely interventions or reevaluations, potentially improving patient management and outcomes.

The remainder of the paper is organized as follows. In Section 2, we define the distribution function of the proposed Sine Log-Logistic (SLL) distribution and derive explicit expressions for its probability density, quantile, and hazard functions. The shape and scale parameters of the SLL distribution are expressed in terms of the median and the $\frac{1}{\sqrt{2}}$th quantile, allowing for consistent plug-in estimation of these parameters. The hazard function exhibits either an inverse bathtub shape or is monotone decreasing depending whether or not the shape parameter exceeds 1. In Subsection 2.1, we fit the proposed SLL distribution, along with the reviewed distributions, to these three datasets. We evaluate their goodness of fit and compare their relative performance using three model selection criteria. Section 3 focuses on the theoretical properties of the proposed SLL distribution. We establish conditions under which the density function is unimodal and determine the existence of its moments. Additionally, we analyze the asymptotic behavior of the hazard function as remission or survival time increases, and examine the regularly varying property of the survival function, which in turn ensure that the distribution of the scaled maximum of n i.i.d. SLL random variables can be approximated by the Fréchet distribution for large n. If the shape parameter exceeds 1, density and the hazard functions of the SLL distribution exhibit an inverse-bathtub shape. The proofs of the main results in Section 3 are provided in the

Appendix.

In Section 4, we estimate the parameters of the proposed SLL distribution using two methods: the plug-in method and maximum likelihood estimation. We also discuss three model selection criteria-Akaike Information Criterion (AIC), Bayesian Information Criterion (BIC), and Consistent Akaike Information Criterion (CAIC). In Section 5, we assess the consistency of the maximum likelihood estimators through Monte Carlo simulation. Finally, in Section 6 we analyze three datasets viz., bladder cancer remission times [26], survival times of head and neck cancer patients [10], and survival times of acute bone cancer patients [16] by using the fitted SLL distribution. The parameter estimates and the p-values from the Kolmogorov-Smirnov (KS) goodness-of-fit test are presented in Tables 2, 3, and 4.

For all three datasets, the estimated values of the shape parameter of the SLL distribution exceed 1. Consequently, the fitted density function and hazard function, as given by equations (3) and (4), are unimodal and exhibit inverse bathtub shape and the hazard decreasing as remission or survival time increases beyond the point at which the hazard peaks for these data. The estimated modal remission and survival times-corresponding to the peaks of the fitted density-are reported in Table 13, representing the most frequent remission or survival durations observed. The peaks of the fitted hazard functions, which indicate the most likely times of recurrence, are also reported in Table 13. The time at which the hazard-the instantaneous rate of relapse-peaks may serve as a critical point for intervention and for planning post-diagnosis and follow-up treatments. We find that the timing of the peak of the density and the hazard function varies significantly across cancer types (see Table 13). For bladder cancer patients, the hazard peaks at approximately 6.7 months into remission. In the case of head and neck cancer, the peak occurs around 50 days following radiotherapy and chemotherapy. For acute bone cancer, the hazard function reaches its peak as early as 7 days after therapy, underscoring the disease's rapid and aggressive progression.

Table 1: *Coefficients of skewness and kurtosis of the three cancer datasets*

Dataset	Skewness	Kurtosis
Remission times of bladder cancer	3.285	18.483
Survival times of head and neck cancer	3.384	16.560
Survival times of acute bone cancer	6.799	51.775

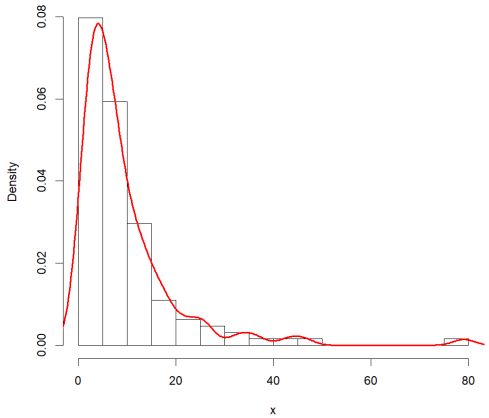

Figure 1: *Histogram and Kernel Density Estimate (KDE) for remission times for bladder cancer*

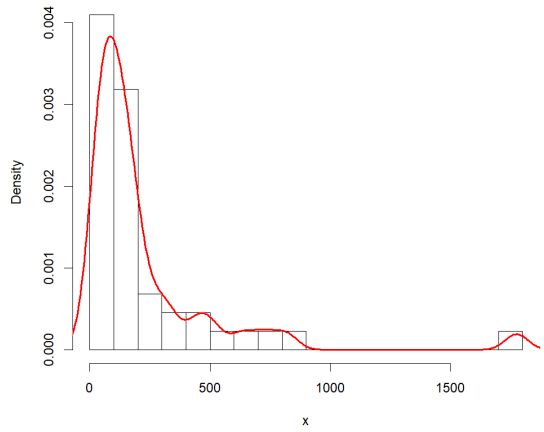

Figure 2: *Histogram and Kernel Density Estimate (KDE) for survival times for head and neck cancer.*

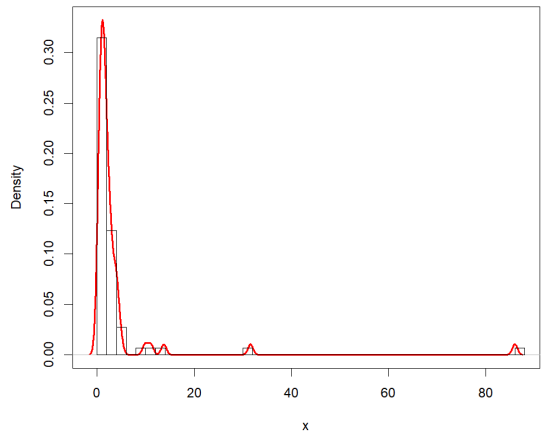

Figure 3: *Histogram and Kernel Density Estimate (KDE) survival times for acute bone cancer.*

2. Sine log-logistic distribution

Let us introduce some notation that will be used throughout the paper. f' denotes the derivative of a differentiable function f. For a real number x, $\lfloor x \rfloor$ denotes the greatest integer less than or equal to x. The notation $\log_2$ refers to the logarithm with base 2. For two functions f and g, $f(x) \sim g(x)$ denotes $\lim_{x\to\infty} \frac{f(x)}{g(x)} = 1$.

We define the new distribution by applying a parsimonious transformation, viz. the sine transformation (also known as SS transformation see [15]), to the distribution function of the log-logistic distribution, which involves two non-negative parameters (viz. α and λ). The choice of the transformation is motivated by [15]. We refer to the resulting new resulting distribution as the sine log-logistic distribution with parameters α and λ and abbreviated as the SLL(α, λ) distribution. The distribution function, density and hazard functions also the quantile function of the SLL(α, λ) distribution turn out to have closed-form expression which are easy to compute and the two parameters, viz. α and λ, turn out to be function functions of two quantiles of this distribution.

Following are the formulae of the distribution function (F), the quantile function (Q), the density function (f) and the hazard function (h) of the proposed SLL distribution

$$F(x) = \begin{cases} \sin\left[\frac{\pi}{2(1+(x/\lambda)^{-\alpha})}\right] & \text{for} \quad x > 0 \\ 0 & \text{otherwise,} \end{cases} \tag{1}$$

where $\alpha,\ \lambda > 0$. α is the shape parameter and λ is the scale parameter.

$$Q(p) = \lambda \left(\frac{1}{\frac{\pi}{2\sin^{-1}(p)} - 1} \right)^{\frac{1}{\alpha}}, \quad 0 < p < 1. \tag{2}$$

$$f(x) = \begin{cases} \frac{\pi\alpha(x/\lambda)^{\alpha-1}}{2\lambda(1+(x/\lambda)^{\alpha})^2} \cos\left[\frac{\pi}{2(1+(x/\lambda)^{-\alpha})}\right] & \text{for} \quad x > 0 \\ 0 & \text{otherwise.} \end{cases} \tag{3}$$

The hazard function of SLL distribution is given by

$$h(x) = \frac{f(x)}{1-F(x)} = \begin{cases} \frac{\pi\alpha(x/\lambda)^{\alpha-1}\cos\left[\frac{\pi}{2(1+(x/\lambda)^{-\alpha})}\right]}{2\lambda(1+(x/\lambda)^{\alpha})^2\left\{1-\sin\left[\frac{\pi}{2(1+(x/\lambda)^{-\alpha})}\right]\right\}} & \text{for} \quad x > 0 \\ 0 & \text{otherwise.} \end{cases} \tag{4}$$

The hazard function (also known as the failure rate) describes the instantaneous risk of failure at a given time, given that the event has not yet occurred up to that time. For instance, in medicine, hazard function describes the instantaneous risk that an event (like death or relapse) will happen at a specific time, given that the patient has survived up to that time.

We plot the PDF (3) and the hazard function (4) of the SLL($\alpha,\ \lambda$) distribution for different values of the shape parameters α and for fixed $\lambda = 1$ in Figures 4 and 5 respectively.

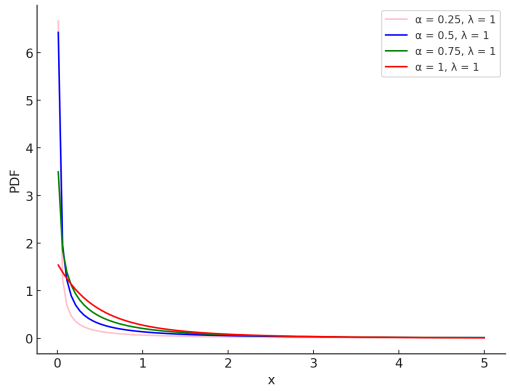

(a) *Plot of the PDF of SLL*$(\alpha, 1)$ *for shape parameter* $\alpha \leq 1$.

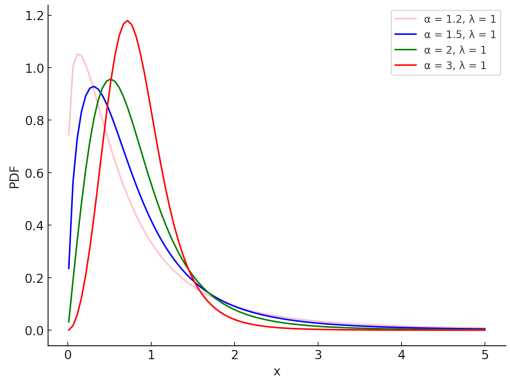

(b) *Plot of the PDF of SLL*$(\alpha, 1)$ *for shape parameter* $\alpha > 1$.

Figure 4: *Plots of the PDF of SLL*$(\alpha, 1)$ *for different values of the shape parameter* α.

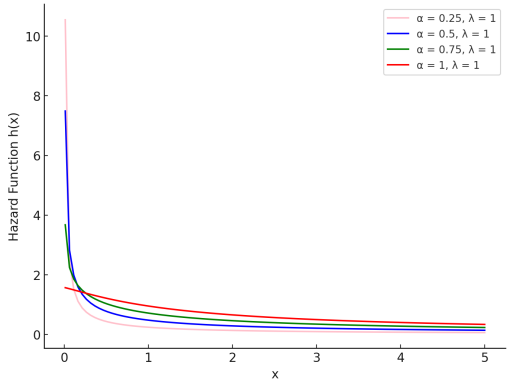

(a) *Plot of the hazard function of* $SLL(\alpha, 1)$ *for shape parameter* $\alpha \leq 1$.

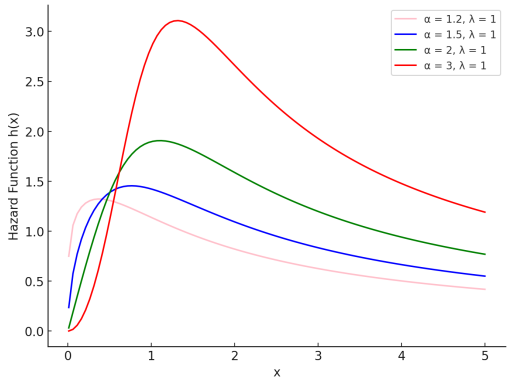

(b) *Plot of the hazard function of* $SLL(\alpha, 1)$ *for shape parameter* $\alpha > 1$.

Figure 5: *Plots of the hazard function of* $SLL(\alpha, 1)$ *for different values of the shape parameter* α.

Equation (2), implies that

$$\lambda = Q\left(\frac{1}{\sqrt{2}}\right), \tag{5}$$

and

$$\alpha = \left(\log_2\left(\frac{Q\left(\frac{1}{\sqrt{2}}\right)}{Q\left(\frac{1}{2}\right)}\right)\right)^{-1}. \tag{6}$$

The scale parameter λ is the $\frac{1}{\sqrt{2}}$th quantile and the shape parameter α is a function of the ratio of the $\frac{1}{\sqrt{2}}$th quantile and the median. Therefore these parameters can be estimated by a plug-in method replacing the quantiles by the sample quantiles.

Remark 1. The PDF (3) of the proposed $SLL(\alpha, \lambda)$ distribution exhibits a long right tail and a unique peak (i.e., it is unimodal) for $\alpha > 1$ (see Figure 4(b)).

In medicine, the mode of the survival time distribution can be interpreted as the most common time point at which treatment failure (e.g., relapse, death, or complication) is most likely to occur. This information may assist in planning follow-up schedules, surveillance intensity, or early intervention strategies.

Remark 2. Figure 5(a) shows that for $\alpha \leq 1$, the hazard function $h(x)$ decreases with increasing x. Figure 5(b) demonstrates that for $\alpha > 1$, the hazard function (4) takes on an inverse bathtub shape, characterized by a long right tail and a single peak or mode.

Probability distributions with an inverse bathtub shape of the hazard function are useful for modeling remission and survival times of various cancers (see [25]). The inverse bathtub shape of the hazard function indicates that the risk of failure in the course of a disease initially increases, reaches a peak, and then decreases as patients recover. For instance, Efron [10] observed that the empirical hazard function of survival times for patients with head and neck cancer is unimodal and resembles an inverse bathtub shape. Further, the mode of the hazard function can be interpreted as the time when the risk of failure is at its peak and can be a useful parameter to identify when a patient is most vulnerable post-diagnosis and treatment.

2.1. Goodness of fit and model selection for the remission and survival time

We fit the proposed $SLL(\alpha,\ \lambda)$ distribution to the remission times of 128 bladder cancer patients reported by Lee and Wang [26], the survival times of head and neck cancer of 44 patients when treated with a combination of radiotherapy and chemotherapy reported by Efron [10], and the

Table 2: *ML estimates, model selection criteria and p-value of KS goodness-of-fit tests for SLL and ten other competing distributions based on remission times of bladder cancer of 128 patients[26].*

Distribution	**ML Estimates**	**AIC**	**BIC**	**CAIC**	p**-value**
SLL	$\hat{\alpha} = 1.403, \hat{\lambda} = 10.342$	823.395	829.099	831.099	0.998
MOEGL	$\hat{\alpha} = 1.079, \hat{\beta} = 0.080, \hat{\theta} = 0.702$	824.621	833.177	836.177	0.862
WC-Weibull	$\hat{\theta} = 0.851, \hat{\gamma} = 0.189$	826.341	832.045	834.045	0.909
EOEHL-LLoGP	$\hat{\alpha} = 2.153, \hat{\lambda} = 0.315, \hat{\theta} = 3.073, \hat{c} = 0.659$	827.300	838.700	842.708	0.997
EPham	$\hat{\alpha} = 0.243, \hat{\sigma} = 2.226, \hat{\gamma} = 8.093$	827.787	836.342	839.343	0.942
EHL-LLoGW	$\hat{\alpha} = 0.861, \hat{\beta} = 0.519, \hat{\delta} = 6.716, \hat{c} = 0.032$	827.800	839.200	834.208	0.997
KGIL	$\hat{\beta} = 0.345, \hat{\lambda} = 9.642, \hat{p} = 4.991, \hat{q} = 3.216$	828.609	840.018	828.935	0.988
GKME	$\hat{\alpha} = 1.374, \hat{\theta} = 0.102$	828.983	834.687	836.687	0.881
M-L	$\hat{\lambda} = 3.268, \hat{\theta} = 24.485, \hat{\beta} = 0.355$	829.156	837.712	840.712	< 0.05
RB-TL-TII-EHL-W	$\hat{\delta} = 24.626, \hat{a} = 0.0001, \hat{b} = 4.008, \hat{\lambda} = 1.270$	830.882	842.290	846.290	0.875
APTEPL	$\hat{\alpha} = 6.279, \hat{\beta} = 11.167, \hat{\delta} = 0.613, \hat{\theta} = 0.752$	831.613	843.021	847.021	0.785
G-SU	$\hat{\phi} = 2.529, \hat{\omega} = 2.961$	852.772	858.476	860.476	0.324

survival times of acute bone cancer patients reported by Mansour et al. [16]. For each data set we compare the fit of SLL distribution to the same for most of the recent probability distributions which have been proposed so far to model these datasets. The parameters are estimated by maximizing the likelihood functions for each dataset. In Tables 2-4, we report maximum likelihood (ML) estimates of the model parameters, the Akaike Information Criterion (AIC), the Bayesian Information Criterion (BIC), and the consistent Akaike Information Criterion (CAIC) [4] scores and the p-value of the Kolmogorov-Smirnov (KS) goodness-of-fit test for each dataset.

Table 3: *ML estimates, model selection criteria and p-value of KS goodness-of-fit tests for SLL and five other competing distributions based on survival times data of head and neck cancer treated with chemeotharapy.*

Distribution	**ML Estimates**	**AIC**	**BIC**	**CAIC**	p**-value**
SLL	$\hat{\alpha} = 1.320, \hat{\lambda} = 222.916$	561.294	564.862	566.862	0.969
MOEGL	$\hat{\alpha} = 0.883, \hat{\theta} = 0.002, \hat{\beta} = 0.038$	561.215	566.567	569.567	0.806
PWS	$\hat{\alpha} = 1.079, \hat{\beta} = 0.080, \hat{\theta} = 0.702$	561.410	566.763	569.763	0.572
G-SU	$\hat{\phi} = 8.622, \hat{\omega} = 11.170$	562.476	566.786	568.045	0.900
DUS-IW	$\hat{\alpha} = 1.119, \hat{\beta} = 57.556$	561.830	565.400	567.398	0.868
APKumW	$\hat{a} = 4.843, \hat{b} = 0.652, \hat{c} = 0.572, \hat{\lambda} = 0.026, \hat{\alpha} = 0.317$	565.1112	565.400	579.032	0.949

Table 4: *ML estimates, model selection criteria and p-value of KS goodness-of-fit tests for SLL and five other competing distributions based on survival times of acute bone cancer.*

Distribution	ML Estimates	AIC	BIC	CAIC	p-value
SLL	$\hat{\alpha} = 1.412, \hat{\lambda} = 2.703$	291.558	296.139	298.139	0.454
MOEGL	$\hat{\alpha} = 1.354, \hat{\theta} = 0.045, \hat{\beta} = 0.001$	288.508	295.380	298.380	0.582
G-SU	$\hat{\phi} = 4.457, \hat{\omega} = 0.765$	285.776	290.357	292.357	0.860
APKumW	$\hat{a} = 5.089, \hat{b} = 0.414, \hat{c} = 0.536, \hat{\lambda} = 1.301, \hat{\alpha} = 0.005$	291.700	303.153	308.153	0.949

The proposed SLL distribution yields good fit to the three datasets on the remission times of 128 bladder cancer patients reported by Lee and Wang [26], the survival times of head and neck cancer of 44 patients reported by Efron [10], and the survival times of 73 acute bone cancer patients reported by Mansour et al. [16] as indicated by the high p-values in the Kolmogorov-Smirnov test for these data. See Tables 2, 3 and 4. Moreover, the proposed SLL distribution outperforms the other candidate distributions in terms of different model selection criteria scores, viz. the AIC, BIC, and CAIC scores for these datasets on remission and survival times of cancer patients reported by Lee and Wang [26], Efron [10] and Mansour et al. [16]. These observations motivate our further research into the mathematical properties of the proposed SLL distribution and the analysis of these three datasets using the proposed model.

3. Properties of the SLL distribution

In this section, we study the mathematical properties of SLL distribution such as moments, hazard function, mode, and regularly varying property of the survival function.

3.1. Moments

Let $X \sim SLL(\alpha, \lambda)$. We have

$$E(X^k) \leq \frac{\pi}{2} \int_0^\infty x^k \frac{\alpha(x/\lambda)^{\alpha-1}}{\lambda(1+(x/\lambda)^\alpha)^2} dx = \frac{\pi}{2} E(Y^k) \tag{7}$$

where Y follows log-logistic distribution with shape parameter $\alpha > 0$ and scale parameter $\lambda > 0$. Since the kth moment of Y exists whenever $k < \alpha$ (see [17]), we obtain the following result.

Theorem 1. The SLL(α, λ) distribution with parameters $\alpha > 0$ and $\lambda > 0$, and PDF given by equation (3), has finite kth moment for all $k < \alpha$.

Corollary 1. For the SLL(α, λ) distribution with $\alpha > 0$ and $\lambda > 0$,

(i) If $\alpha > 1$, then the mean exists and is finite.

(ii) If $\alpha > 2$, then both the mean and variance exist and are finite.

3.2. Mode of the SLL Distribution

The mode of a probability distribution is the value at which its PDF attains the maximum, representing the most favorable outcome [25]. The mode can be a more appropriate alternative to the mean, especially when the data are skewed or contain outliers. In survival analysis, the mode determines the most common point at which failure is most likely to occur. For example, in studies involving remission and survival times of cancer patients, the mode indicates the most probable time at which failure events such as relapse or death might occur.

We now state a theorem that establishes the existence and uniqueness of the mode of the SLL distribution, determined by the value of the shape parameter α. The proof is provided in the appendix.

Theorem 2. The SLL(α, λ) distribution with parameters $\alpha > 0$ and $\lambda > 0$, and PDF given by equation (3), satisfies the following:

(i) If $0 < \alpha \leq 1$, then the mode does not exist.

(ii) If $\alpha > 1$, then the distribution has a unique mode $x_M \in (0, x^*)$ where $x^* = \lambda \left(\frac{\alpha-1}{\alpha+1}\right)^{1/\alpha}$.

3.3. Hazard Function

In survival analysis, the hazard function h(x) also known as the failure rate describes the instantaneous rate at which an event (such as death, relapse, or failure) occurs, given that the subject has survived up to time x (see [25]). In medical research, the hazard function plays a crucial role in determining the risk dynamics over time and is widely used, particularly in analyzing survival data. The mode of the hazard function, or the point at which it attains its maximum, indicates the most likely time of failure, conditional on survival up to that time can guide clinical decisions regarding the timing of interventions or monitoring.

The following lemmas describe the asymptotic behavior of the hazard function $h(x)$, given in (4), for the SLL(α, λ) distribution. We refer to the appendix for the proofs.

Lemma 1. The hazard function $h(x)$ given in (4) for the SLL(α, λ) distribution, with $\alpha, \lambda > 0$, satisfies the following property:

$$\lim_{x\to\infty} h(x) = 0. \tag{8}$$

Lemma 2. Let F be a continuous distribution function supported on $[0, \infty)$ with a differentiable density f. Suppose that:

- f is inverse bath-tub shaped; that is, there exists $t^* \geq 0$ such that f is increasing on $[0, t^*]$ and decreasing on $[t^*, \infty)$,
- the hazard rate function $h(x) = \frac{f(x)}{1-F(x)}$ satisfies $\lim_{x\to\infty} h(x) = 0$.

Then h is inverse bath-tub shaped; that is, there exists $t^{**} \geq t^*$ such that h is increasing on $[0, t^{**}]$ and decreasing on $[t^{**}, \infty)$.

Remark 3. Lemma 1 and 2 imply that for $\alpha > 1$ the hazard function h of SLL(α, λ) distribution will be inverse bath-tub shaped and the peak of the hazard function will be to the right of the mode.

3.4. Regularly Varying Survival Function and asymptotic distribution of the extreme remission or survival time

In the study of survival analysis and extreme value theory, the concept of regular variation plays a major role in understanding the asymptotic behavior of tail distributions (see [9]). A survival function that is regularly varying at infinity exhibits a heavy-tailed property, implying that the probability of extreme or rare events decays at a polynomial rate. In that case, the maximum survival time distribution can be approximated by the Fréchet distribution. Moreover, in studies involving the remission and survival times of cancer patients, the tail behavior of survival distributions helps assess long-term risks and the persistence of chronic diseases.

Definition 1. A Lebesgue-measurable function $f : (0, \infty) \to \mathbb{R}$ is said to be *regularly varying at infinity with index* $\alpha \in \mathbb{R}$ if

$$\lim_{x\to\infty} \frac{f(tx)}{f(x)} = t^\alpha, \quad \text{for all } t > 0. \tag{9}$$

In this case, we write $f \in \mathrm{RV}_\alpha$.

The following result establishes that the survival function of the SLL distribution possesses the property of regular variation, with the detailed proof presented in the appendix.

Theorem 3. The survival function $\bar{F}(x) = 1 - F(x)$ of the SLL(α, λ) distribution with $\alpha, \lambda > 0$ is regularly varying at infinity with index -2α, i.e.,

$$\bar{F} \in \mathrm{RV}_{-2\alpha}.$$

Next we obtain the asymptotic distribution of centered and scaled $M_n = \max(X_1, \ldots, X_n)$ where $X_1, \ldots, X_n$ are independently and identically distributed (i.i.d.) random variables following $SLL(\alpha, \lambda)$.

Definition 2. Let $X_1, \ldots, X_n$ be i.i.d. random variables with a distribution function F. Then F is said to be in the maximum domain of attraction (MDA) of a non-degenerate distribution function H if there exist sequences of real numbers (c_n) and (d_n) with $c_n > 0$ for all $n \in \mathbb{N}$ such that the following holds:

$$\lim_{n\to\infty} \mathbb{P}\left(\frac{M_n - d_n}{c_n} \leq x\right) = \lim_{n\to\infty} F^n(c_n x + dn) = H(x)$$

for every continuity point x of H. We write $F \in MDA(H)$ to denote that F is in the maximum domain of attraction of H.

Definition 3. The Fréchet distribution with parameter $\xi > 0$ is defined by the following distribution function:

$$H_\xi(x) = exp\left(-(1+\xi x)^{-\frac{1}{\xi}}\right), \quad 1 + \xi x > 0. \tag{10}$$

Theorem 4 (see [9].)**.** For $\xi > 0$, $F \in MDA(H_\xi)$ if and only if $1 - F$ is regularly varying at infinity with index $-1/\xi$.

From Theorem 3 and 4, we have the following result:

Theorem 5. Let $X_1, \ldots, X_n$ be i.i.d. random variables following $SLL(\alpha, \lambda)$, where $\alpha, \lambda > 0$ with df F. Then

$$\lim_{n\to\infty} \mathbb{P}\left(\frac{M_n}{c_n} \leq x\right) = \lim_{n\to\infty} F^n(c_n x) = H_{1/2\alpha}(x), \quad 1 + x/2\alpha > 0$$

where c_n is the $(1 - \frac{1}{n})$th quantile of $SLL(\alpha, \lambda)$.

Remark 4. The scaled maxima M_n of i.i.d. random variables following $SLL(\alpha, \lambda)$, where $\alpha, \lambda > 0$ is well approximated by the Fréchet distribution with distribution function $H_{1/2\alpha}(x)$ for large n.

4. Estimation of Parameters SLL Distribution

In this section we estimate the parameters of the proposed distribution by two methods, namely the plug-in method and the likelihood function maximization methods and we discuss the three model selection criteria viz., AIC, BIC and CAIC.

4.1. Plug-in Method

We use the quantile function of the SLL distribution given in equation (1.2) to estimate the parameters of the SLL distribution. From equations (1.3) and (1.4), we observe that the parameters of the proposed distribution can be expressed in terms of the quantiles. Given a dataset, plug-in estimators of the parameters are obtained by replacing the quantiles in (1.2) by the corresponding sample quantiles in the given data. The following theorem esnures strong consistency of the plug-in estimators.

Theorem 6. Let $X_1, X_2, \ldots, X_n$ be independently and identically distributed (i.i.d.) random variables following the $SLL(\alpha, \lambda)$ distribution. Then, the estimators

$$\widehat{\lambda} = X_{\left(\left\lfloor \frac{n}{\sqrt{2}} \right\rfloor + 1\right)} \tag{11}$$

and

$$\widehat{\alpha} = \left(\log_2 \left(\frac{X_{\left(\left\lfloor \frac{n}{\sqrt{2}} \right\rfloor + 1\right)}}{X_{\left(\left\lfloor \frac{n}{2} \right\rfloor + 1\right)}} \right) \right)^{-1} \tag{12}$$

are strongly consistent estimators of λ and α.

4.2. Model Selection and Maximum Likelihood Estimation

Let $X_1, \ldots, X_n$ be i.i.d. continuous random variables with PDF $f(x; \boldsymbol{\theta})$, with parameter vector $\boldsymbol{\theta} \in \mathbb{R}^k$. The log-likelihood function is given by

$$L(\boldsymbol{\theta}) = \sum_{i=1}^{n} \ln f(X_i; \boldsymbol{\theta}). \tag{13}$$

Let $\hat{\boldsymbol{\theta}}$ be the maximum likelihood (ML) estimate of the parameter vector $\boldsymbol{\theta}$ and $L(\hat{\boldsymbol{\theta}})$ is the maximized log-likelihood function (13).

The log-likelihood function is used in evaluating the modeling selection criteria. Following are the well known model selection criteria based on log-likelihood function.

1. **Akaike Information Criterion (AIC):** The AIC, proposed by Akaike (see [4]), is defined as

   $$\text{AIC} = -2L(\hat{\boldsymbol{\theta}}) + 2k,$$

   where k is the number of estimated parameters in the model.

2. **Bayesian Information Criterion (BIC):** The BIC, also known as the Schwarz Information Criterion (see [18]), is given by

   $$\text{BIC} = -2L(\hat{\boldsymbol{\theta}}) + k \ln(n),$$

   where n is the sample size. BIC favors parsimonious models by imposing a larger penalty for model complexity compared to AIC.

3. **Consistent Akaike Information Criterion (CAIC):** The CAIC (see [4]) is defined as

   $$\text{CAIC} = -2L(\hat{\boldsymbol{\theta}}) + k\left[\ln(n) + 1\right].$$

   Similar to BIC, CAIC also favors parsimonious models by imposing a larger penalty for the number of parameters.

Let $X_1, \ldots, X_n$ be i.i.d. random variables from the $SLL(\alpha, \lambda)$ distribution with $\alpha, \lambda > 0$. The log-likelihood function is given by

$$L(\alpha, \lambda) = n \ln\left(\frac{\pi\alpha}{2\lambda}\right) + \sum_{i=1}^{n} \ln\left[\frac{\left(\frac{X_i}{\lambda}\right)^{\alpha-1}}{\left(1 + \left(\frac{X_i}{\lambda}\right)^{\alpha}\right)^2}\right] + \sum_{i=1}^{n} \ln\left[\cos\left(\frac{\pi}{2\left(1 + \left(\frac{X_i}{\lambda}\right)^{-\alpha}\right)}\right)\right]. \tag{14}$$

The estimating equations of the parameters of $SLL(\alpha, \lambda)$ are obtained by equating the partial derivatives of the log-likelihood function with respect to the parameters to zero i.e,

$$\frac{\partial L}{\partial \alpha} = 0, \frac{\partial L}{\partial \lambda} = 0.$$

Closed-form solutions of the estimating equations cannot be obtained, we use numerical methods to compute the ML estimates of the parameters. Specifically, we minimize the negative log-likelihood function (14) numerically using the L-BFGS-B method available in R.

In Figures 6, 7 and 8 we present the three-dimensional plots of the log-likelihood function (14) for the remission times of bladder cancer [26] and the survival times of head and neck cancer [10], respectively. From these figures, we observe that the log-likelihood function for the SLL distribution in both datasets exhibits a unique maximum.

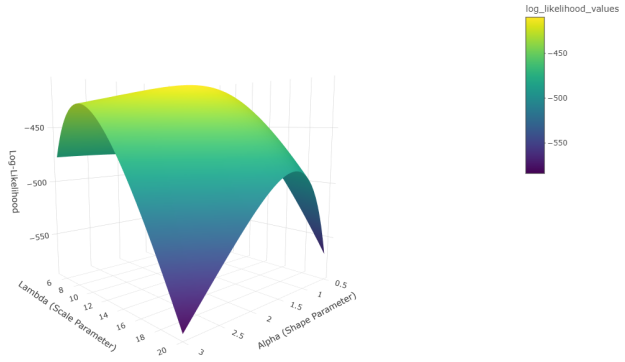

Figure 6: *3D plot of the log-likeihood function for the SLL distribution for Bladder cancer remission times*

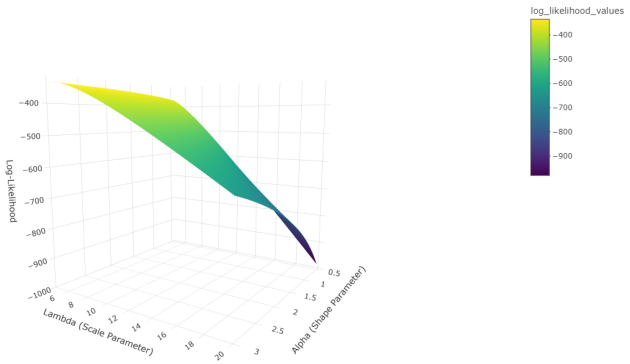

Figure 7: *3D plot of the log-likeihood function for the SLL distribution for survival times of head and neck cancer*

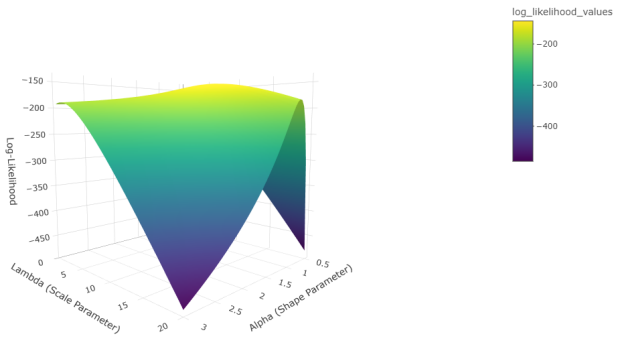

Figure 8: *3D plot of the log-likeihood function for the SLL distribution for Survival times of acute bone cancer*

The log-likelihood function is an important function that helps in evaluating the model selection criteria such as AIC, BIC, and CAIC, as discussed below.

5. Simulation and Real Data Analysis

5.1. Mone-Carlo Simulation.

In this section, we conduct the Monte Carlo simulation method to assess the consistency of ML estimates for the parameters involved in the proposed SLL distribution.

We use the quantile function of the $SLL(\alpha, \lambda)$ given in equation (1.2) to generate $N = 1000$ random samples of varying sizes ($n = 50, 100, 250, 500, 1000$) for different values of the true parameters α, λ (see Tables 5 – 12).we consider cases where the true value of the shape parameter satisfies $\alpha \leq 1$ while in Tables 9–12, we examine scenarios where $\alpha > 1$. In all cases, the scale parameter is fixed at $\lambda = 1$.

We present the mean ML estimates ($\widehat{\alpha}$) and ($\widehat{\lambda}$) of the parameters along with the corresponding root mean squared errors (RMSE) in Tables 5, 6, and 7. The RMSE of a parameter θ is defined as follows:

$$RMSE(\hat{\theta}) = \sqrt{\frac{1}{n}\sum_{i=1}^{n}(\hat{\theta}_i - \theta)^2}. \tag{15}$$

Table 5: *Mean MLEs and RMSEs of parameters α and λ for the SLL distribution over 1000 simulations. True parameter values are $\alpha = 0.25$ and $\lambda = 1$.*

Sample Size	**Mean** $\hat{\alpha}$	**Mean** $\hat{\lambda}$	**RMSE**(α)	**RMSE**(λ)
50	0.257	1.252	0.033	1.200
100	0.253	1.162	0.022	0.700
250	0.251	1.065	0.013	0.390
500	0.251	1.012	0.009	0.248
1000	0.250	1.012	0.006	0.179

Table 6: *Mean MLEs and RMSEs of parameters α and λ for the SLL distribution based on 1000 simulations. True parameter values are $\alpha = 0.5$ and $\lambda = 1$.*

Sample Size	**Mean** $\hat{\alpha}$	**Mean** $\hat{\lambda}$	**RMSE**($\hat{\alpha}$)	**RMSE**($\hat{\lambda}$)
50	0.515	1.034	0.066	0.429
100	0.506	1.040	0.044	0.288
250	0.502	1.016	0.027	0.181
500	0.501	0.998	0.018	0.121
1000	0.501	1.002	0.012	0.088

Table 7: *Mean MLEs and RMSEs of parameters α and λ for the SLL distribution over 1000 simulations. True parameter values are $\alpha = 0.75$ and $\lambda 1$.*

Sample Size	**Mean** $\hat{\alpha}$	**Mean** $\hat{\lambda}$	**RMSE**(α)	**RMSE**(λ)
50	0.772	1.005	0.099	0.270
100	0.759	1.018	0.067	0.185
250	0.752	1.007	0.040	0.119
500	0.752	0.997	0.027	0.080
1000	0.752	1.000	0.019	0.058

Table 8: *Mean MLEs and RMSEs of parameters α and λ for the SLL distribution over 1000 simulations. True parameter values are $\alpha = 1$ and $\lambda = 1$.*

Sample Size	**Mean** $\hat{\alpha}$	**Mean** $\hat{\lambda}$	**RMSE**(α)	**RMSE**(λ)
50	1.029	0.997	0.132	0.200
100	1.012	1.010	0.089	0.137
250	1.003	1.004	0.054	0.088
500	1.003	0.997	0.036	0.060
1000	1.002	1.000	0.025	0.044

Table 9: *Mean MLEs and RMSEs of parameters α and λ for the SLL distribution over 1000 simulations. True parameter values are $\alpha = 1.2$ and $\lambda = 1$.*

Sample Size	**Mean** $\hat{\alpha}$	**Mean** $\hat{\lambda}$	**RMSE**(α)	**RMSE**(λ)
50	1.235	0.995	0.158	0.165
100	1.214	1.007	0.106	0.114
250	1.204	1.003	0.065	0.074
500	1.203	0.998	0.043	0.050
1000	1.203	1.000	0.030	0.036

Table 10: *Mean MLEs and RMSEs of parameters α and λ for the SLL distribution over 1000 simulations. True parameter values are $\alpha = 1.5$ and $\lambda = 1$.*

Sample Size	**Mean** $\hat{\alpha}$	**Mean** $\hat{\lambda}$	**RMSE**(α)	**RMSE**(λ)
50	1.544	0.994	0.197	0.132
100	1.518	1.005	0.133	0.090
250	1.505	1.002	0.081	0.059
500	1.504	0.997	0.054	0.040
1000	1.503	1.000	0.037	0.029

Table 11: *Mean MLEs and RMSEs of parameters α and λ for the SLL distribution over 1000 simulations. True parameter values are $\alpha = 2$ and $\lambda = 1$.*

Sample Size	**Mean** $\hat{\alpha}$	**Mean** $\hat{\lambda}$	**RMSE**(α)	**RMSE**(λ)
50	2.059	0.994	0.263	0.099
100	2.024	1.003	0.178	0.068
250	2.007	1.001	0.109	0.044
500	2.005	0.998	0.072	0.030
1000	2.004	1.000	0.050	0.022

Table 12: *Mean MLEs and RMSEs of parameters α and λ for the SLL distribution over 1000 simulations. True parameter values are $\alpha = 3$ and $\lambda = 1$.*

Sample Size	**Mean** $\hat{\alpha}$	**Mean** $\hat{\lambda}$	**RMSE**(α)	**RMSE**(λ)
50	3.088	0.995	0.396	0.066
100	3.036	1.001	0.266	0.050
250	3.010	1.001	0.162	0.029
500	3.008	0.999	0.107	0.020
1000	3.007	1.000	0.075	0.015

Remark 5. The results in Tables 5–12 the RMSE of the ML estimates of parameters decreases

toward zero with increasing sample size n, indication consistency of the ML estimators for α and λ.

5.2. Data Analysis

In this section, we analyze three datasets viz., remission times (in months) of 128 bladder cancer patients, survival times (in days) of 44 head and neck cancer patients treated with both radiotherapy and chemotherapy [10] and survival times (in days) 73 acute bone cancer patients [16] by using the fitted SLL$(\alpha,\ \lambda)$ distribution. From Tables 2, 3, and 4, we observe that for all the three datasets the estimated value of shape parameter α exceed 1, and hence the corresponding density and hazard functions are inverted bathtub shaped. See Figures 10, 11, 13, 14, 16, and 17. Figures 9 - 17 display the Q-Q plots, hazard functions, and the KDEs alongside the fitted PDFs of the SLL distribution for the bladder cancer remission times, head and neck cancer survival times, and acute bone cancer survival times. For each dataset, we estimate the mode, median, and peak of the hazard function based on the fitted SLL distribution. The mode and the peak of the hazard function are obtained numerically by maximizing the fitted PDF and hazard function. These estimated statistics are summarized in Table 13. The findings for each dataset are outlined below:

- The fitted hazard functions exhibit inverted bathtub shape for all the three data sets, indicating the rate of recurrence or death for each of the three types of cancer patients first increase, reaches a peak and then decrease with increasing remission or survival time. However the peak remission or survival times are drastically different for the three types of cancer.
- **Remission Times Bladder Cancer:**
  For this dataset, the estimated modal remission time is 2.6 months, while the peak of the estimated hazard function occurs at 6.7 months. This indicates that the highest risk of relapse of the bladder cancer arises approximately four months after the most common remission period of 2.6 months. The estimated median remission time is 6.3 months.
- **Survival Times of Head and Neck Cancer:**
  The modal survival time for this dataset is approximately 45 days, while the peak of the hazard function function occurs at around 50 days, which indicate a short period of elevated mortality risk during 45 to 50 days after radiotherapy and chemotherapy and thus the need for intensive monitoring and support during this period.
- **Survival Times of Acute Bone Cancer:**
  For this dataset, the estimated modal survival time is approximately 2.5 days, highlighting a very short typical survival period. The peak of the hazard function occurs at around 7 days, while the median survival time is estimated to lie between 6 and 6.5 days. These findings suggest that the highest risk of mortality arises shortly within a week the most typical survival time, emphasizing the aggressive nature of the cancer.

Table 13: *Estimated mode, median, and mode of the hazard function using the fitted SLL distribution for bladder cancer, head and neck cancer, and acute bone cancer datasets*

Cancer Type	Mode	Median	Mode of Hazard Function
Bladder Cancer	2.6 (months)	6.3 (months)	6.7 (months)
Head and Neck Cancer	45 (days)	131.8 (days)	50 (days)
Acute Bone Cancer	2.6 (days)	6.3(days)	6.8 (days)

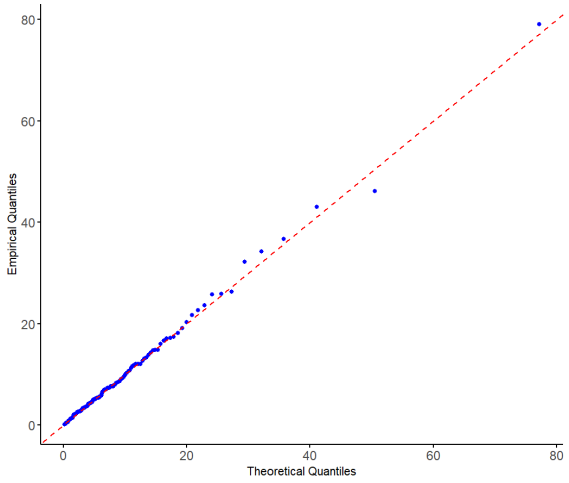

Figure 9: *Q-Q plot for the bladder cancer remission times data*

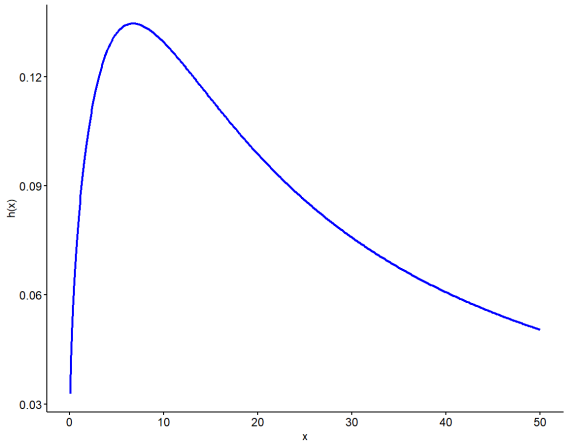

Figure 10: *Plot of hazard function of the fitted SLL distribution for the bladder cancer remission times data*

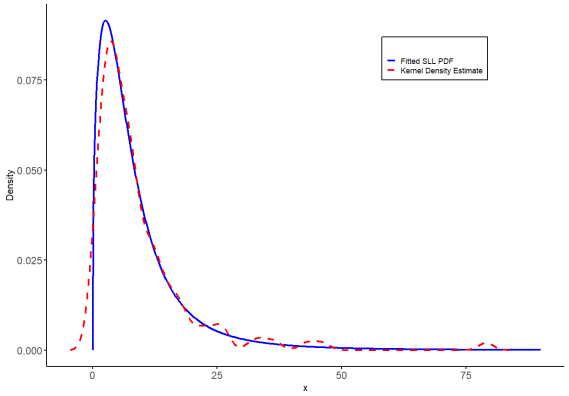

Figure 11: *Plot of the fitted SLL density along with the KDE plot for the bladder cancer remission times data*

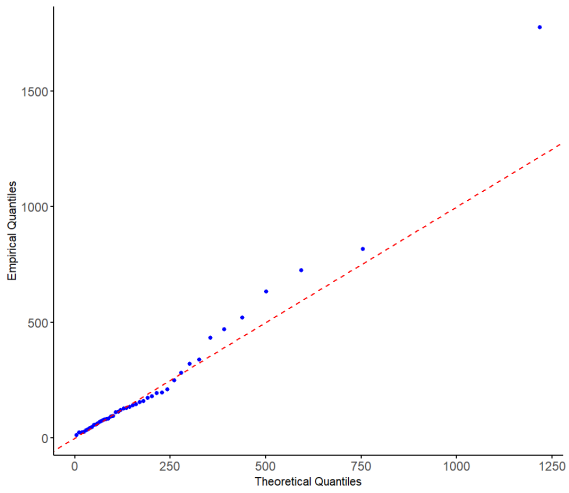

Figure 12: *Q-Q plot for the the survival times of head and neck cancer data*

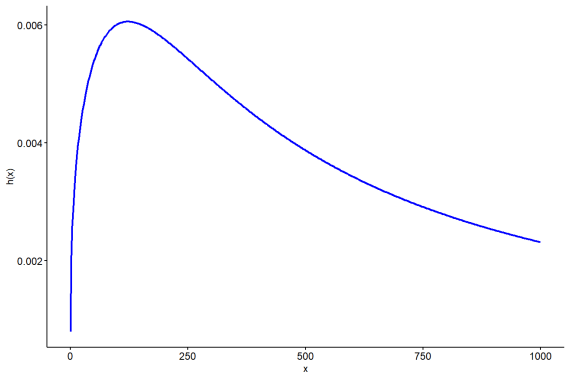

Figure 13: *Plot of hazard function of the fitted SLL distribution for the the survival times of head and neck cancer data*

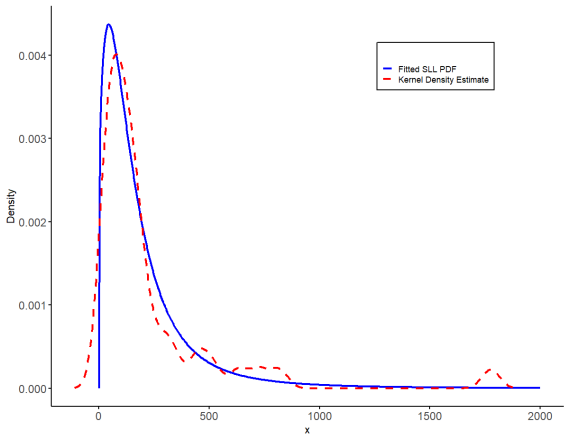

Figure 14: *Plot of the fitted SLL density along with the KDE plot for the the survival times of head and neck cancer data*

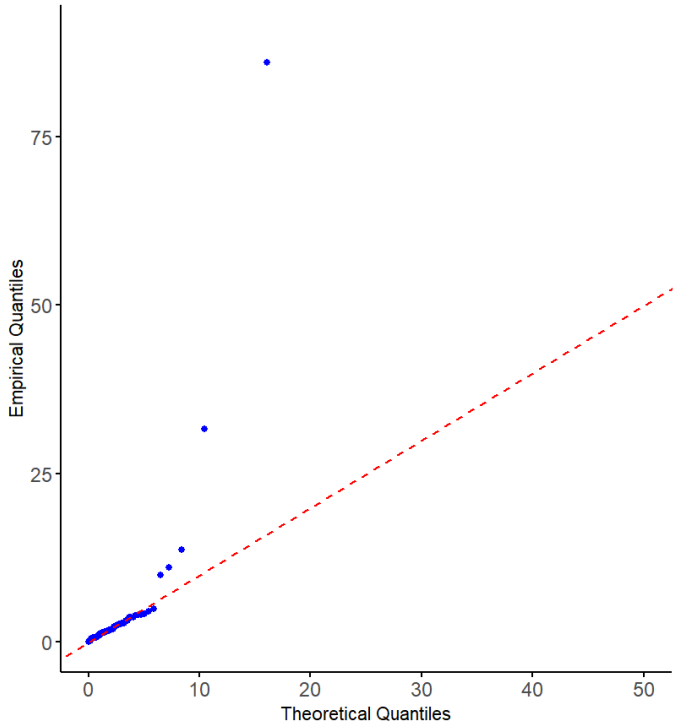

Figure 15: *Q-Q plot for the the survival times acute bone cancer*

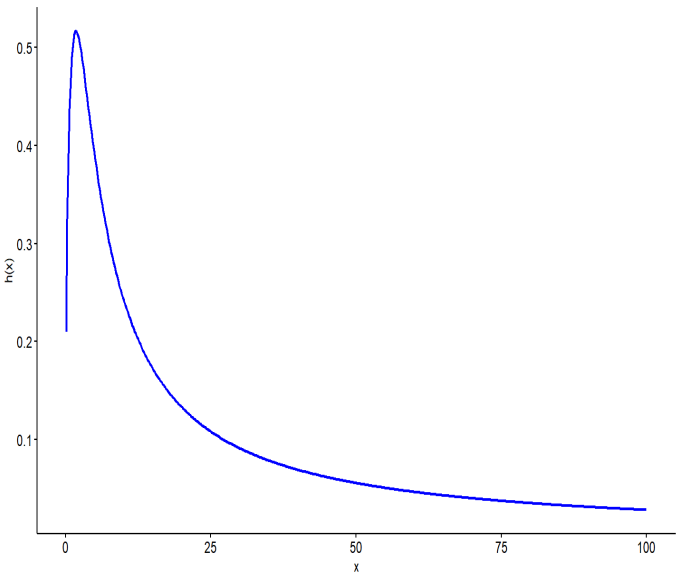

Figure 16: *Plot of hazard function of the fitted SLL distribution for the the survival times acute bone cancer*

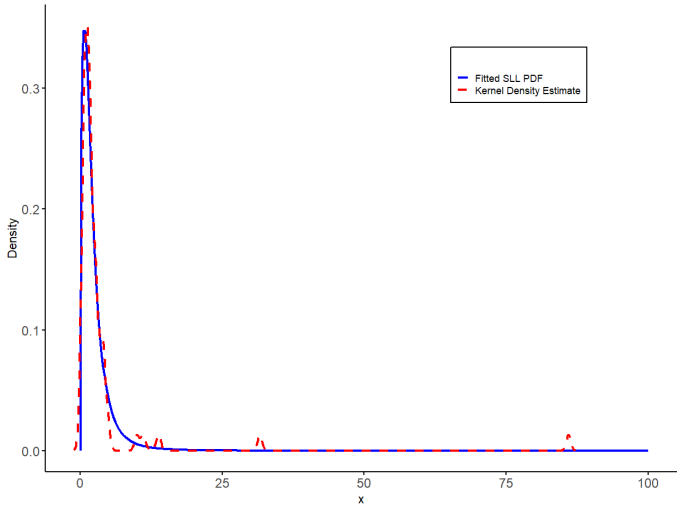

Figure 17: *Plot of the fitted SLL density along with the KDE plot for the the survival times acute bone cancer*

Funding

The first author was supported by Council of Scientific & Industrial Research, Government of India under the CSIR-JRF scheme (Grant No. 09/796(0121)/2021-EMR-I). The author thanks the funding agency for the financial assistance.

Declarations

The authors declare that they have no conflict of interest.

References

[1] Alotaibi, R., Nassar, M., & Elshahhat, A. (2024). A new extended Pham distribution for modelling cancer data. *Journal of Radiation Research and Applied Sciences*, **17**(3), 100961.
[2] Abiodun, A. A., & Ishaq, A. I. (2022). On Maxwell-Lomax distribution: Properties and applications. *Arab Journal of Basic and Applied Sciences*, **29**(1), 221-232.
[3] Alzaatreh, A., Lee, C., & Famoye, F. (2013). A new method for generating families of continuous distributions. *Metron*, **71**(1), 63-79.
[4] Anderson, D. R., Burnham, K. P., & White, G. C. (1998). Comparison of Akaike information criterion and consistent Akaike information criterion for model selection and statistical inference from capture-recapture studies. *Journal of Applied Statistics*, **25**(2), 263-282.
[5] Benkhelifa, L. (2017). The Marshall-Olkin extended generalized Lindley distribution: Properties and applications. *Communications in Statistics-Simulation and Computation*, **46**(10), 8306-8330.
[6] Chamunorwa, S., Makubate, B., Oluyede, B., & Chipepa, F. (2021). The exponentiated half logistic-log-logistic Weibull distribution: Model, properties and applications. *Journal of Statistical Modelling: Theory and Applications*, **2**(1), 101-120.
[7] Colleoni, M., Bonetti, M., Coates, A. S., et al. (2000). Early start of adjuvant chemotherapy may improve treatment outcome for premenopausal breast cancer patients with tumors not expressing estrogen receptors. *Journal of Clinical Oncology*, **18**(3), 584-590.
[8] Collett, D. (2023). *Modelling Survival Data in Medical Research.* Chapman and Hall/CRC.
[9] de Haan, L., & Ferreira, A. (2006). *Extreme value theory: An introduction*. Springer Science & Business Media.

[10] Efron, B. (1988). Logistic regression, survival analysis, and the Kaplan-Meier curve. *Journal of the American Statistical Association*, **83**(402), 414-425.
[11] Eissa, F. Y., & Sonar, C. D. (2023). Alpha power transformed extended power Lindley distribution. *Journal of Statistical Theory and Applications*, **22**(1), 1-18.
[12] Gauthami, P., & Chacko, V. M. (2021). DUS transformation of inverse Weibull distribution: An upside-down failure rate model. *Reliability: Theory & Applications*, **16**(2 (62)), 58-71.
[13] Kavya, P., & Manoharan, M. (2023). A new lifetime model for non-monotone failure rate data. *Journal of the Indian Society for Probability and Statistics*, **24**(2), 211-241.
[14] Klakattawi, H. S. (2022). Survival analysis of cancer patients using a new extended Weibull distribution. *PLOS ONE*, **17**(2), e0264229.
[15] Kumar, D., Singh, U., & Singh, S. K. (2015). A new distribution using sine function-Its application to bladder cancer patients data. *Journal of Statistics Applications & Probability*, **4**(3), 417.
[16] Mansour, M., Yousof, H. M., Shehata, W. A., & Ibrahim, M. (2020). A new two parameter Burr XII distribution: properties, copula, different estimation methods and modeling acute bone cancer data. *Journal of Nonlinear Science and Applications*, **13**(5), 223-238.
[17] Mendoza, N. V., Ortega, E. M., & Cordeiro, G. M. (2016). The exponentiated-log-logistic geometric distribution: Dual activation. *Communications in Statistics - Theory and Methods*, **45**(13), 3838-3859.
[18] Neath, A. A., & Cavanaugh, J. E. (2012). The Bayesian information criterion: Background, derivation, and applications. *Wiley Interdisciplinary Reviews: Computational Statistics*, **4**(2), 199-203.
[19] Ray, M., & Shanker, R. (2024). A probability model for survival analysis of cancer patients. *Reliability: Theory & Applications*, **19**(3 (79)), 78-94.
[20] Mudholkar, G. S., & Srivastava, D. K. (1993). Exponentiated Weibull family for analyzing bathtub failure-rate data. *IEEE Transactions on Reliability*, **42**(2), 299-302.
[21] Odhah, O. H., Alshanbari, H. M., Ahmad, Z., & Rao, G. S. (2023). A weighted cosine-G family of distributions: Properties and illustration using time-to-event data. *Axioms*, **12**(9), 849.
[22] Ogunde, A. A., Chukwu, A. U., & Oseghale, I. O. (2023). The Kumaraswamy generalized inverse Lomax distribution and applications to reliability and survival data. *Scientific African*, **19**, e01483.
[23] Oluyede, B., & Moakofi, T. (2023). The gamma-Topp-Leone-type II-exponentiated half logistic-G family of distributions with applications. *Stats*, **6**(2), 706-733.
[24] Oluyede, B., Chipepa, F., & Wanduku, D. (2021). Exponentiated half logistic-power generalized Weibull-G family of distributions: Model, properties and applications. *Eurasian Bulletin of Mathematics*, **3**(3), 134-161.
[25] Lawless, J. F. (2003). *Statistical Models and Methods for Lifetime Data* (2nd ed.). Hoboken, New Jersey: John Wiley & Sons.
[26] Lee, E. T., & Wang, J. (2003). *Statistical methods for survival data analysis*. John Wiley & Sons.
[27] Rannona, K., Oluyede, B., Chipepa, F., & Makubate, B. (2022). The exponentiated odd exponential half logistic-G power series class of distributions with applications. *Journal of Statistics and Management Systems*, **25**(8), 1821-1848.
[28] Shanker, R., & Shukla, K. K. (2023). Power weighted Sujatha distribution with properties and application to survival times of patients of head and neck cancer. *Reliability: Theory & Applications*, **18**(3 (74)), 568-581.

Appendix

Proof of Theorem 2:

The probability density function of the SLL distribution is given by

$$f(x) = \frac{\pi}{2} g(x) \cos\left(\frac{\pi}{2} G(x)\right), \quad x > 0,$$

where $g(x)$ and $G(x)$ are the PDF and df of the log-logistic distribution:

$$g(x) = \frac{(\alpha/\lambda)(x/\lambda)^{\alpha-1}}{[1+(x/\lambda)^{\alpha}]^2}, \quad G(x) = \frac{1}{1+(x/\lambda)^{-\alpha}}.$$

Differentiating $f(x)$, we obtain:

$$f'(x) = \frac{\pi}{2}g'(x)\cos\left(\frac{\pi}{2}G(x)\right) - \frac{\pi^2}{4}g(x)^2\sin\left(\frac{\pi}{2}G(x)\right).$$

The derivative of $g(x)$ is:

$$g'(x) = \frac{g(x)}{x\,(1+(x/\lambda)^{\alpha})}\left[\alpha - 1 - (\alpha+1)(x/\lambda)^{\alpha}\right].$$

Case I: $0 < \alpha \leq 1$

In this case, the expression in brackets is negative for all $x > 0$, implying $g'(x) < 0$. Therefore, $f'(x) < 0$ for all $x > 0$, so $f(x)$ is strictly decreasing on $(0, \infty)$. Moreover, since $g(x) \to \infty$ as $x \to 0$, it follows that $f(x) \to \infty$ as $x \to 0$. Thus, $f(x)$ is unbounded near 0 and strictly decreasing afterwards, implying no mode exists in $(0, \infty)$.

Case II: $\alpha > 1$

In this case, the function $g'(x) = 0$ has a unique solution

$$x^* = \lambda\left(\frac{\alpha-1}{\alpha+1}\right)^{1/\alpha},$$

with $g'(x) > 0$ for $x < x^*$, and $g'(x) < 0$ for $x > x^*$. To find the critical points of $f(x)$, define the function:

$$k(x) = \tan\left(\frac{\pi}{2}G(x)\right) - \frac{2g'(x)}{\pi g(x)^2}.$$

Then $f'(x) = 0$ if and only if $k(x) = 0$. As $x \to 0$, $g(x) \to 0$, $g'(x)/g(x)^2 \to \infty$, and hence $k(x) \to -\infty$. At $x = x^*$, $g'(x^*) = 0$, so $k(x^*) = \tan\left(\frac{\pi}{2}G(x^*)\right) > 0$. One can show that $k'(x) > 0$ in $(0, x^*)$, so $k(x)$ is strictly increasing in this interval.

By the Intermediate Value Theorem, there exists a unique $x_M \in (0, x^*)$ such that $k(x_M) = 0$, hence $f'(x_M) = 0$. Moreover, the sign change of $f'(x)$ from positive to negative at x_M confirms that this is a unique maximum of $f(x)$, i.e., the mode.

Proof of Lemma 1:

We define

$$\theta(x) := \frac{\pi}{2\left(1+\left(\frac{x}{\lambda}\right)^{-\alpha}\right)}$$

and

$$\varepsilon(x) := \frac{\pi}{2} - \theta(x) = \frac{\pi}{2}\left(1 - \frac{1}{1+\left(\frac{x}{\lambda}\right)^{-\alpha}}\right).$$

As $x \to \infty$, we have

$$\varepsilon(x) \sim \frac{\pi}{2}\left(\frac{x}{\lambda}\right)^{-\alpha}.$$

Now, as $\varepsilon(x) \to 0$, we have the following approximations:

$$\cos[\theta(x)] = \cos\left[\frac{\pi}{2} - \varepsilon(x)\right] = \sin[\varepsilon(x)] \sim \varepsilon(x) \sim \frac{\pi}{2}\left(\frac{x}{\lambda}\right)^{-\alpha}$$

$$1 - \sin[\theta(x)] = 1 - \sin\left[\frac{\pi}{2} - \varepsilon(x)\right] = 1 - \sin[\varepsilon(x)] \sim \frac{1}{2}\varepsilon(x)^2 \sim \frac{\pi^2}{8}\left(\frac{x}{\lambda}\right)^{-2\alpha}$$

Therefore, for large x, the hazard function given in (4) can be approximated as

$$h(x) \sim \frac{\frac{\pi^2\alpha}{2}\left(\frac{x}{\lambda}\right)^{-1}}{\frac{\pi^2}{4}\lambda} = \frac{4\alpha}{\lambda^2}\cdot\frac{1}{x}.$$

Hence,

$$\lim_{x\to\infty} h(x) = 0.$$

Proof of Lemma 2:

Since f is differentiable, the hazard function $h(x) = \frac{f(x)}{1-F(x)}$ is differentiable.
Differentiating h gives

$$h'(x) = \frac{f'(x)(1-F(x)) + f(x)^2}{(1-F(x))^2}.$$

The sign of $h'(x)$ is determined by the numerator

$$N(x) = f'(x)(1-F(x)) + f(x)^2.$$

On $[0, t^*]$, $f'(x) \geq 0$ and $f(x)^2 \geq 0$, so $N(x) \geq 0$, implying $h'(x) \geq 0$. Thus, h is increasing on $[0, t^*]$.

If h continues to increase or remain constant on $[t^*, \infty)$, h would be bounded below by $h(t^*)$ and non-decreasing beyond t^*, so $h(x)$ could not converge to zero as $x \to \infty$, contradicting the assumption that $\lim_{x\to\infty} h(x) = 0$.

Thus, there must exist $t^{**} \geq t^*$ such that h is increasing on $[0, t^{**}]$ and decreasing on $[t^{**}, \infty)$, indicating that h is inverse bath-tub shaped.

Proof of Theorem 3:

We define

$$\theta(x) := \frac{\pi}{2\left(1+\left(\frac{x}{\lambda}\right)^{-\alpha}\right)},$$

and

$$\varepsilon(x) := \frac{\pi}{2} - \theta(x) = \frac{\pi}{2}\left(1 - \frac{1}{1+\left(\frac{x}{\lambda}\right)^{-\alpha}}\right).$$

As $x \to \infty$, we have

$$\varepsilon(x) \sim \frac{\pi}{2}\left(\frac{x}{\lambda}\right)^{-\alpha}.$$

Therefore, for large x, we have the following approximation of the survival function of the SLL(α, λ) distribution

$$\bar{F}(x) \sim \frac{1}{2}\left(\frac{\pi}{2}\left(\frac{\lambda}{x}\right)^{\alpha}\right)^2 = \frac{\pi^2}{8}\left(\frac{\lambda}{x}\right)^{2\alpha}.$$

Thus, as $x \to \infty$,

$$\bar{F}(x) \sim \frac{\pi^2}{8}\lambda^{2\alpha}x^{-2\alpha}.$$

Since $\bar{F}(x) \sim Cx^{-2\alpha}$ for some constant $C > 0$, it follows that

$$\lim_{x\to\infty}\frac{\bar{F}(tx)}{\bar{F}(x)} = t^{-2\alpha}, \quad \text{for all } t > 0.$$

Therefore, the survival function $\bar{F}(x)$ is *regularly varying at infinity* with index -2α, that is,

$$\bar{F}(x) \in \mathrm{RV}_{-2\alpha}.$$